J. Korean Inst. Electr. Electron. Mater. Eng.
Vol. 38, No. 4, pp. 366-375 July 2025
doi: https://doi.org/10.4313/JKEM.2025.38.4.3
ISSN 1226-7945(Print), 2288-3258(Online)

Tutorial Status Report

각설탕 템플릿을 활용한 압전 다공성 스펀지 제작 및 특성 분석

이예빈[1,2], 김현승[1,3], 엄태욱[1,2], 정창규[1,2,3]

[1] 전북대학교 신소재공학부 전자재료공학전공
[2] 전북대학교 JBNU-KIST 산학연융합학과
[3] 전북대학교 에너지저장변환공학과 대학원

초록: 압전 특성을 가지는 다공성 고분자 구조체는 기계적 자극을 전기 신호로 변환할 수 있는 특성을 바탕으로 생체 재료 및 조직공학 응용 분야에서 주목받고 있다. 그러나 기존의 다공성 구조체 제작 공정은 기공 구조의 제어, 구조적 일관성 유지, 공정 재현성 확보 측면에서 한계를 보이며 복잡한 공정 조건을 필요로 하는 경우가 많다. 이러한 문제를 해결하기 위해 본 연구에서는 설탕 입자를 압축 성형한 각설탕을 기공 템플릿으로 활용하여 다공성 Poly (vinylidene fluoride) (PVDF) 압전 스펀지를 쉽고 재현성 있게 제작하는 공정을 제안한다. 각설탕 템플릿의 입자 크기를 조절함으로써 스펀지의 기공 크기와 분포를 효과적으로 제어할 수 있으며, 균일한 개방 기공 네트워크를 형성할 수 있다. 제작된 스펀지는 설탕 입도 차이에 따른 기공 구조 및 분포, 기계적 거동과 압전 특성을 중심으로 평가되었으며, 이를 통해 구조체의 물성과 기능적 유효성을 확인하였다. 본 연구는 간단하면서도 재현성 높은 다공성 구조체 제작 전략과 함께 정량적 분석 방법을 제시함으로써, 압전 고분자 기반 생체재료 플랫폼 개발에 있어 공정 접근성과 실용성을 향상시킬 수 있을 것으로 기대된다.

키워드: 다공성 PVDF 스펀지, 압전, 각설탕 템플릿, 용액 기반 제조, 기공 크기 제어

Fabrication and Characterization of Piezoelectric Porous Sponge Using Sugar Cubes

Yebin Lee[1,2], Hyunseung Kim[1,3], Tauk Eom[1,2], and Chang Kyu Jeong[1,2,3]

[1] Division of Advanced Materials Engineering, Jeonbuk National University, Jeonju 54896, Korea
[2] Department of JBNU-KIST Industry-Academia Convergence Research, Jeonbuk National University, Jeonju 54896, Korea
[3] Department of Energy Storage/Conversion Engineering of Graduate School, Jeonbuk National University, Jeonju 54896, Korea

(Received May 10, 2025; Revised June 6, 2025; Accepted June 9, 2025)

Abstract: Porous polymeric structures with piezoelectric properties have attracted considerable attention in the fields of biomaterials and tissue engineering due to their ability to convert mechanical stimuli into electrical signals. However, conventional fabrication methods for porous structures often face limitations in controlling pore architecture, maintaining structural uniformity, and achieving process reproducibility, in addition to requiring complex processing conditions. To address these issues, we propose a facile and reproducible fabrication method for porous poly (vinylidene fluoride) (PVDF) piezoelectric sponges using molded sugar cubes as sacrificial pore templates. By adjusting the particle size of the sugar templates, the pore size and distribution of the sponges could be effectively controlled, and a uniform open-pore network was achieved. The fabricated sponges were evaluated with a focus on pore morphology, mechanical behavior, and piezoelectric performance depending on the sugar particle size, and these evaluations confirmed the structural properties and functional efficacy. This study presents a simple and reproducible fabrication strategy along with a quantitative analysis method for porous structures, which is expected to enhance process accessibility and practical applicability in the development of piezoelectric polymer-based biomaterial platforms.

Keywords: Porous PVDF sponge, Piezoelectric, Sugar-cube templating, Solution-based fabrication, Pore size control

✉ **Chang Kyu Jeong; ckyu@jbnu.ac.kr**

1. INTRODUCTION

Piezoelectric materials can convert mechanical deformation into electrical potential or induce mechanical deformation in response to electrical stimuli [1–4]. These properties originate from their crystal structure or molecular chains possessing a non-centrosymmetric arrangement [5]. Lead zirconate titanate (PZT), a representative inorganic ceramic piezoelectric material, has been widely used due to its excellent piezoelectric properties, however, its lead content raises concerns regarding biocompatibility and environmental safety [6]. Consequently, lead-free piezoelectric ceramics such as barium titanate (BTO) and potassium sodium niobate (KNN) have been actively investigated [7]. However, these materials typically suffer from low flexibility and high brittleness, leading to growing interest in polymer-based piezoelectric materials that offer superior flexibility and biocompatibility [8].

Poly (vinylidene fluoride) (PVDF), a representative polymeric piezoelectric material, is a ferroelectric polymer that can form a β-phase through processes such as thermal treatment to align its molecular chains, resulting in high spontaneous polarization and excellent piezoelectric performance [9–12]. In addition, PVDF exhibits flexibility, processability, chemical stability, and biocompatibility, making it a promising material for a wide range of electronic and biomedical applications, including wearable sensors, implantable medical devices, and scaffolds for tissue regeneration [13–16].

One structural strategy to further expand the applicability of PVDF involves the incorporation of porous architecture. Porous structures offer advantages such as enhanced mechanical flexibility, reduced weight, increased surface area, and improved sensitivity to vibration. In biomedical applications, porous structures provide favorable environments for cell attachment, infiltration, proliferation, and angiogenesis. Pore structures enable physiological processes such as fluid exchange, oxygen and nutrient transport, and waste removal in wound healing and tissue regeneration platforms. Porous scaffolds with piezoelectric properties can further contribute to tissue regeneration by converting mechanical deformations arising from external or physiological stimuli–such as body movements, muscle contractions, and blood flow-into electrical signals that stimulate cells [17,18]. For porous structures to be suitable for tissue engineering, they possess open-pore architectures with interconnected internal and external pathways, macropores ranging from tens to hundreds of micrometers, and sufficient mechanical stability to allow the free transport of cells, nutrients, and bodily fluids [19–21]. Although various fabrication methods for porous structures have been studied each with its own advantages, they generally fall short of satisfying all the requirements simultaneously [22].

For instance, electrospinning offers a high surface area and flexible fibrous networks, but the resulting structures are typically thin and lack uniformity and well-defined three-dimensional pore architectures [23]. Salt leaching and gas foaming are relatively simple processes capable of producing three-dimensional structures, yet they struggle to precisely control pore size and distribution, often resulting in irregular or closed pores that hinder interconnectivity. Freeze-drying can yield relatively uniform internal pore connectivity but is highly sensitive to external variables such as cooling rate, resulting in poor reproducibility and mechanically fragile structures. Moreover, most of the previously proposed methods are optimized for nanoscale porosity, making it difficult to create microscale environments necessary for tissue regeneration. This limitation may hinder functional recovery processes such as cell migration, vascularization, and nerve regeneration. Therefore, a simple and highly reproducible fabrication method that enables simultaneous control over pore size, distribution, interconnectivity, and structural stability is required [24].

In this study, we propose a simple and reproducible fabrication process for porous structures using sugar particles compressed into cube shapes as environmentally friendly and low-cost templates. The process involves immersing the sugar cubes into a polymer solution, allowing the solution to infiltrate the inter-particle boundaries, and then removing the sugar to form a continuous open-pore structure. This approach enables the formation of a uniform three-dimensional network with interconnected pores throughout the structure, and the pore size can be tuned to the microscale range suitable for cell infiltration by adjusting the size of the sugar particles [25]. Using this sugar-cube templating method, porous piezoelectric sponges composed of PVDF are fabricated, and the pore morphology, mechanical properties, and piezoelectric performance are systematically analyzed according to the template conditions, with the aim of enhancing process accessibility in the development of piezoelectric polymer-based porous biomaterials.

2. VARIOUS FABRICATION METHODS FOR FORMING POROUS STRUCTURES

Various fabrication techniques have been proposed for the formation of porous structures, each influencing the resulting pore size, morphology, distribution, and interconnectivity [26]. Particle leaching involves mixing water-soluble particles such as sodium chloride into a polymer solution, forming a structure, and then removing the particles to generate a porous network [27]. While this method is relatively simple and does not require expensive equipment, it has limitations in that the pore structure can become non-uniform depending on the size and distribution of the particles used [28]. Phase separation-based techniques induce phase separation within the polymer solution and subsequently remove the solvent to form a fine porous structure [29]. In particular, thermally induced phase separation (TIPS) allows control over pore size and distribution through regulation of cooling rate and concentration, and directional TIPS enables the formation of oriented pore structures by controlling the cooling direction [30,31]. However, the resulting pore sizes are generally small, and the degree of structural control is limited. Freeze-drying involves freezing a polymer solution or aqueous slurry, followed by solvent sublimation under vacuum to generate a porous structure [32,33]. This process can achieve good pore interconnectivity, but it is sensitive to external factors such as temperature during freezing and sublimation, often resulting in poor reproducibility, non-uniform structures, or mechanically fragile porous scaffolds [34].

Gas foaming forms pores by introducing high-pressure gas into the polymer or by generating gas through chemical reactions within the matrix [35]. This method avoids the use of organic solvents and enables porous structure formation; however, it tends to produce closed pores, making it difficult to ensure interconnectivity [36]. Melt molding involves mixing polymers with a porogen such as polyvinyl alcohol (PVA), which can be decomposed by solvent or heat, molding the mixture under heat and pressure, and then removing the porogen. It allows the fabrication of structures in various shapes and sizes without the use of solvents; however, the polymer may melt and form a film on the surface during molding, resulting in a non-porous outer layer [37,38]. Electrospinning applies a high voltage to a polymer solution to produce fibers with micro- to nanoscale diameters, which are deposited to form porous mats. This method allows precise control over fiber diameter and yields high surface area, but the resulting structure is typically two-dimensional and lacks sufficient pore interconnectivity [39].

For three-dimensional structure fabrication, design-based approaches such as 3D printing have been explored [40]. Although complex pore architectures can be realized through digital modeling and layer-by-layer depositions, challenges remain including the limited range of printable polymers and relatively low resolution [41]. It should be noted that reported fabrication methods each offer unique advantages and limitations and have been selectively applied depending on the intended application. However, in the context of tissue engineering and biomaterial applications, technical improvements are still needed in terms of pore size control, interconnectivity, mechanical stability, and process reproducibility [42].

3. FABRICATION PROCESS OF POROUS PVDF SPONGES USING SUGAR-CUBE TEMPLATES

The porous PVDF sponge fabrication method proposed in this study which utilizes sugar-cube templates, is like the particle leaching technique, as it forms pores using water-soluble particles in a polymer solution. However, unlike conventional particle dispersion, this method involves compressing and molding sugar particles into a dense template, thereby enhancing structural uniformity. The sugar-cube templates were designed to enable control over the final pore size of the structure by adjusting the particle size of the sugar. Sugar was selected as the template material due to its favorable characteristics for shape control. In contrast, salt is hygroscopic and readily absorbs moisture from the air, and its crystalline morphology is irregular, making it difficult to form uniform structures when used as a template. On the other hand, sugar particles have relatively uniform shapes and are less susceptible to deformation from moisture absorption, allowing them to maintain their form stably throughout the process and making them well-suited as templates [43]. To this end, commercially available sugar was finely ground using a mortar or grinder and then sieved sequentially using meshes with different diameters (e.g., 500 μm and 150 μm) to classify it into various particle size ranges (Fig. 1(a)). A small amount

of water was added to the sugar to form a slurry, which was then uniformly compressed in a mold to fabricate sugar cubes of the desired shape (Fig. 1(b)). The molded sugar cubes were thoroughly dried at room temperature for more than 24 hours to prevent further dissolution from residual moisture and to ensure the mechanical integrity of the templates.

The fabrication of porous PVDF sponges consists of three main steps: preparation of the polymer solution, immersion of the template and thermal treatment, and removal of the template followed by drying of the structure (Fig. 2(a)). The polymer solution was prepared by dissolving PVDF in a mixed solvent of acetone and N, N-dimethylformamide (DMF). Using mixed solvent of acetone and DMF was intended to balance the solubility of PVDF and the structural stability of the sugar-cube template. When using only DMF leads to dissolving sugar template. Furthermore, if the solution evaporates too quickly, surface hardening occurs before the internal structure forms; conversely, if it evaporates too slowly, structural formation may be delayed, and residual solvent may cause collapse of the template [39]. To resolve the trade-off between PVDF solubility and sugar template stability, the proportion of acetone was deliberately increased to minimize template degradation while ensuring adequate dissolution of PVDF. This optimized solvent composition enabled the preparation of a solution with suitable viscosity and evaporation kinetics, thereby promoting the formation of a structurally stable and uniformly porous architecture. The sugar-cube templates were fully immersed in the PVDF solution and subjected to low-temperature heating for over 12 hours to allow gradual solvent evaporation, enabling the PVDF to infiltrate between sugar particles and form the structure. A secondary thermal treatment was then conducted to promote the formation of the β-phase in PVDF, thereby enhancing its piezoelectric properties. After the structure was formed, it was immersed in flowing water for more than 6 hours to completely dissolve the sugar, resulting in porous sponge with a continuous open-pore network. Finally, the porous structure was dried at room temperature for 24 hours to remove any residual solvent and moisture from the internal structure. Figure 2(b) presents photographs of the fabricated porous PVDF sponges. The sponges have a thickness of approximately 2.5 mm and exhibit notable flexibility.

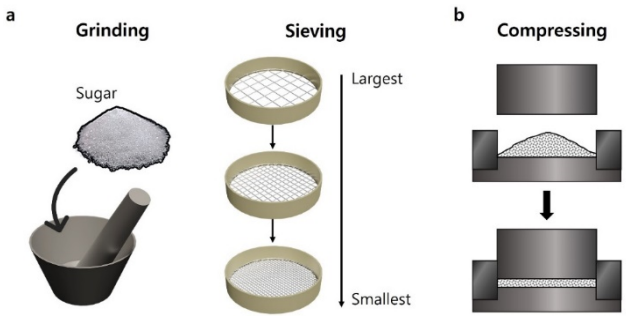

Fig. 1. Schematic illustration of the (a) sugar particle classification process and (b) sugar particle compression molding process.

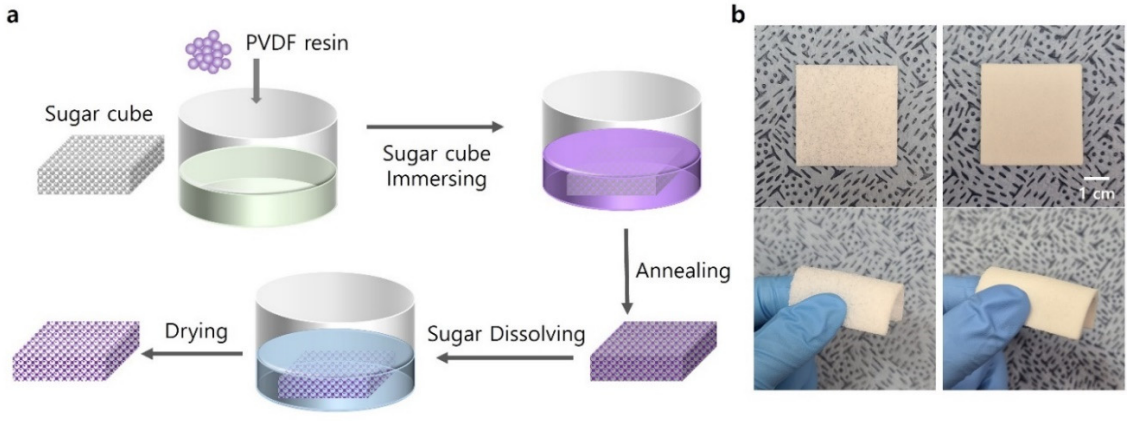

Fig. 2. (a) Schematic illustration of the fabrication process of the PVDF sponge and (b) photographs of PVDF sponges fabricated with different sugar cube templates. Granulated sugar cube template base PVDF sponge (left), Superfine sugar cube template base PVDF sponge (right).

4. CHARACTERIZATION AND DISCUSSION OF POROUS PVDF SPONGES

4.1 Morphological and Structural Analysis

To investigate the effect of sugar particle size on the pore structure of porous PVDF sponges, various techniques were employed to analyze pore morphology, as well as the continuity and interconnectivity of the internal structure. Figure 3(a) presents an optical microscopy (OM) image taken at 5× magnification, in which sugar particles were thinly spread on a slide glass to achieve uniform distribution on the surface. The particles with sizes in the range of 300-500 μm were classified as granulated sugar, while those in the range of 50-150 μm were defined as superfine sugar. Figure 3(b) shows cross-sectional scanning electron microscopy (SEM) images of porous PVDF sponges fabricated using granulated sugar and superfine sugar as templates, respectively. To prevent charge accumulation, the surface of the non-conductive PVDF samples was sputter-coated with Pt, and the structural uniformity and pore morphology were compared at 50× magnification. Pore size analysis was conducted using the ImageJ software, where more than five random regions were selected from SEM images taken at the same magnification for measurement. The analysis revealed that the average pore size of sponges templated with granulated sugar was approximately 200-400 μm, while that of sponge templated with superfine sugar was approximately 25-100 μm.

These results demonstrate that the pore size of PVDF sponges can be effectively controlled by adjusting the particle size of the sugar used as the template. The observation that the pore size was smaller than the original sugar particle size can be attributed to particle size reduction during sugar-cube fabrication or to the shrinkage of pore boundaries as the PVDF solution filled the interstitial spaces between particles. Figure 3(c) illustrates the internal structure of the porous PVDF sponges visualized in three dimensions using micro-computed tomography (Micro-CT). Scanning was conducted at a resolution of 20 μm, and the obtained data were reconstructed into 3D models using CTvox software. The results confirmed that both samples possessed continuous and uniform open-pore networks. These structural characteristics are attributed to the use of rigid sugar-cube templates and suggest the potential for enhanced structural control compared to conventional fabrication methods.

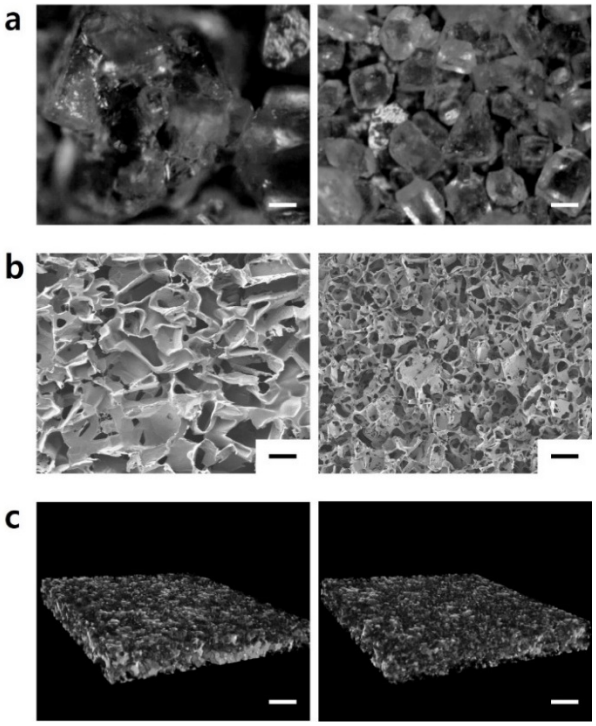

Fig. 3. (a) OM images of sugar particles, (b) SEM, and (c) Micro-CT images of PVDF sponges fabricated with different sugar cube templates. Granulated sugar cube template based (left) and superfine sugar cube template based (right). Scale bars are 100 μm in (a), 200 μm in (b) and 2 mm in (c), respectively.

4.2 Crystalline and Molecular Structure Analysis

The piezoelectric properties of PVDF-based sponges are primarily determined by the formation of the β-phase crystalline structure, which is closely related to the degree of molecular chain alignment and crystallinity. PVDF can exhibit various crystalline phases, including α, β, and γ; among these, the β-phase characterized by the alignment of all dipoles in the same direction exhibits superior piezoelectric [9]. In this study, thermal treatment was conducted near the Curie temperature of PVDF, which is considered an optimal condition to maximize crystallization while preserving dipole alignment [44].

Accordingly, X-ray diffraction (XRD) and Fourier-transform infrared (FT-IR) spectroscopy were performed to

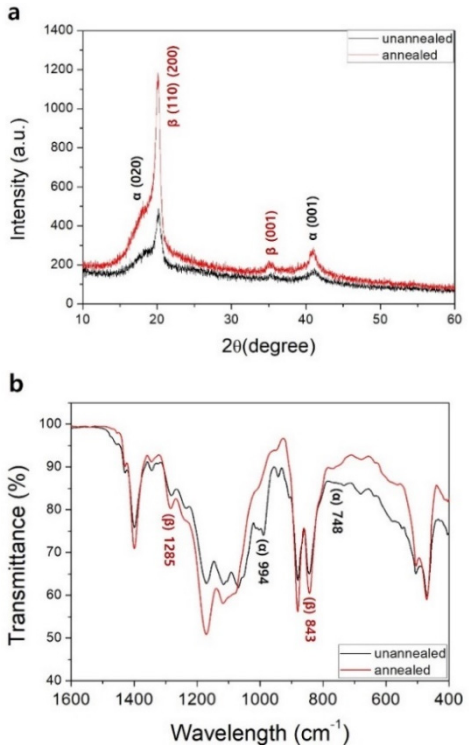

Fig. 4. (a) XRD and (b) FT-IR spectra of PVDF sponges under different annealing conditions.

investigate phase changes induced by thermal treatment during the sponge fabrication process. For XRD analysis, sponge samples were cut and pressed flat onto a sample holder to maintain surface uniformity, and measurements were conducted within a 2θ range of 10-60˚ with a step size of 0.02˚, comparing the crystalline structure before and after thermal treatment. As shown in Fig. 4(a), the intensity of diffraction peaks corresponding to the characteristic β-phase crystal planes (110) and (200) increased significantly after thermal treatment [45,46].

FT-IR spectra were acquired in the range of 400-1600 cm^{-1}, and the spectral differences between samples before and after thermal treatment were compared (Fig. 4(b)). After thermal treatment, the peaks near 843 cm^{-1} and 1285 cm^{-1} associated with the β-phase increased, whereas the peaks around 748 cm^{-1} and 994 cm^{-1} corresponding to the α-phase were reduced [47,48]. Both XRD and FT-IR results consistently indicate an increase in β-phase content, confirming that thermal treatment effectively promotes molecular alignment and β-phase crystallization in porous PVDF sponges, thereby enhancing their piezoelectric performance.

4.3 Mechanical Property Analysis

The mechanical properties of porous PVDF sponges are closely related to the mechanical stability of the cellular microenvironment in applications such as tissue engineering scaffolds and implantable biomaterials, making the evaluation of tensile and compressive resistance essential. Therefore, to analyze the influence of pore structures formed by different sugar particle sizes on the mechanical behavior of the sponges, tensile and compression tests were conducted using a universal testing machine (UTM) [49–51]. All tests were carried out at a loading rate of 100 μm/min.

Figure 5(a) presents the tensile stress-strain curves of porous PVDF sponges fabricated using granulated and superfine sugar-cube templates. The tensile test specimens were cut to dimensions of 40 mm × 5 mm with a thickness of 2.5 mm, and both ends were fixed to the grips of a vertical clamp jig for uniaxial tensile loading. The sponge templated with granulated sugar exhibited a maximum tensile stress of approximately 30 kPa and a maximum strain of about 60%. The curve displayed repetitive stress drops, indicating that microcracks formed along the pore boundaries under tensile loading and gradually propagated and accumulated, ultimately leading to structural failure. The sponge templated with superfine sugar showed a higher maximum tensile stress of approximately 100 kPa but exhibited a relatively lower maximum strain of around 20%. The corresponding stress-strain curve showed a rapid initial stress increase followed by sudden fracture, reflecting the characteristic of densely packed small pores that effectively transmit stress, enhancing strength but limiting strain accommodation.

Figure 5(b) presents the compressive stress-strain curves of the porous PVDF sponges. Compression test specimens were prepared with dimensions of 10 mm × 10 mm and 2.5 mm in thickness, and compressive force was applied vertically using a flat-plate jig. The sponge based on granulated sugar showed a maximum compressive stress of approximately 2 MPa with a relatively gradual stress increase. This is attributed to the cushioning effect of the pores, which absorb external loads and reduce structural resistance. The sponge templated with superfine sugar exhibited a higher maximum compressive stress of approximately 4.5 MPa, with stress increasing rapidly as strain progressed. This indicates that the densely distributed pore structure effectively disperses the load and alleviates

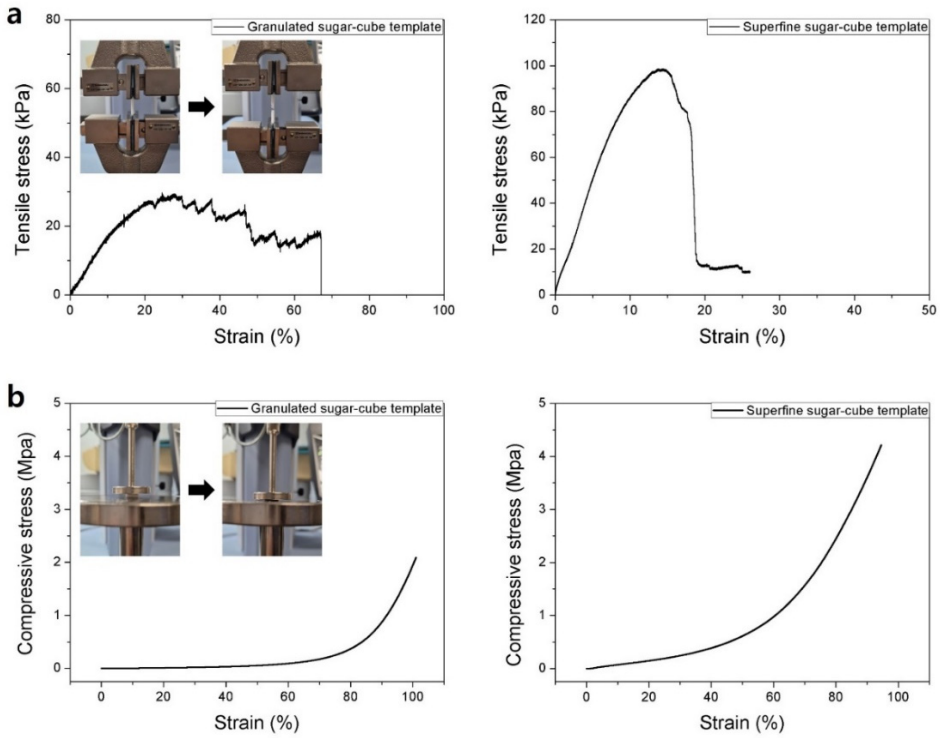

Fig. 5. (a) Tensile and (b) compressive stress-strain curves of PVDF sponges fabricated with different sugar cube templates. Photographic image of experimental setup (inset). Granulated sugar cube template base PVDF sponge (left) and superfine sugar cube template base PVDF sponge (right).

stress concentration, thereby enhancing the overall structural integrity. These differences in mechanical behavior demonstrate that mechanical properties can be tailored through pore structure control, providing experimental evidence for designing stable structures suitable for biomedical environments.

4.4 Piezoelectric Performance Analysis

To evaluate the potential of PVDF sponges as bioelectrical stimulation platforms capable of promoting cell proliferation, differentiation, and migration in addition to their structural advantages, quantitative analysis of piezoelectric properties was conducted. The device for output measurement was designed such that the electrode layers and the internal PVDF sponge shared the same porous architecture, thereby maintaining continuity in the porous structure. Silver nanowires, selected for their high electrical conductivity and excellent interfacial adhesion, were utilized as surface electrodes [52]. These were applied via a dip-coating process that enabled uniform deposition throughout the porous structure preserving the internal continuity of the sponge [53,54]. The device consisted of untreated PVDF sponge samples with electrode layers attached to the top and bottom surfaces. For stable signal extraction, copper lead wires were inserted at the center of each electrode layer and connected using silver paste to establish electrical contact with the measurement equipment (Fig. 6(a)) [55]. Output measurements were conducted by applying periodic mechanical stimuli using a pressing machine under conditions of 10 N pressure at a frequency of 1 Hz (Fig. 6(b)).

Figure 6(c) and (d) present the piezoelectric performance of PVDF sponges fabricated using granulated and superfine sugar-cube templates, respectively. The recorded peak-to-peak voltage outputs were approximately 1.5 V and 2 V, and the corresponding current outputs were about 20 nA and 40 nA, respectively. These values are consistent with the piezoelectric coefficients measured using a d_{33} meter, which were -28.4 pC/N for the granulated sugar-based sponge and -30.6 pC/N for the superfine sugar-based sponge. The sponge

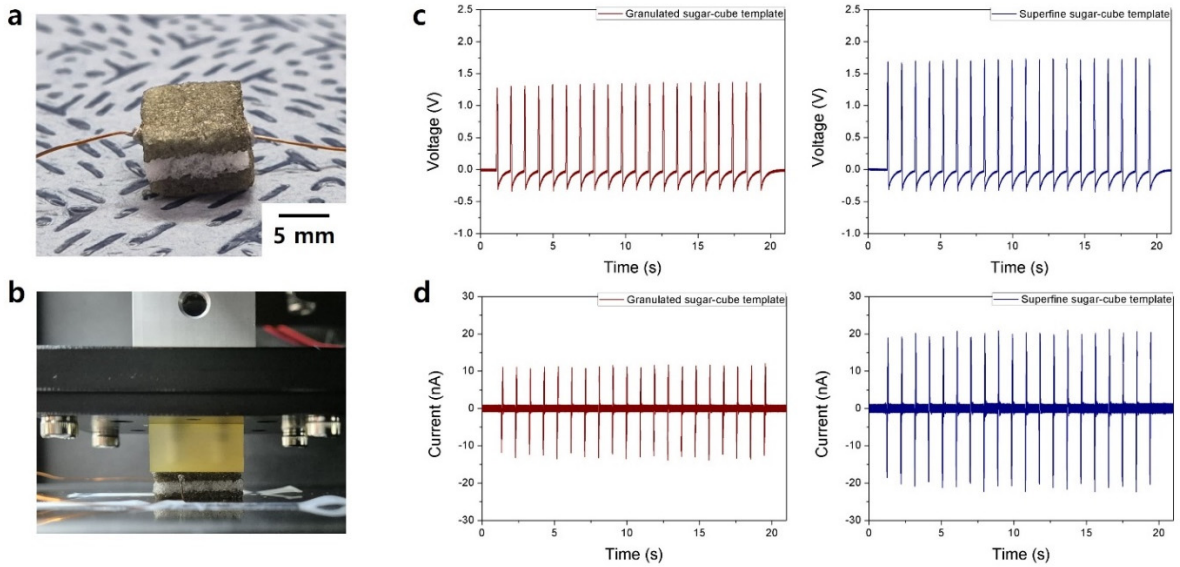

Fig. 6. Piezoelectric output performance of PVDF sponges under press-release stimulation. Photographic image of (a) device and (b) experimental setup. (c) Output voltage and (d) current signals of PVDF sponges fabricated with different sugar cube templates. Granulated sugar cube template base PVDF sponge (left) and superfine sugar cube template base PVDF sponge (right).

based on superfine sugar exhibited higher output performance due to its denser pore structure, which facilitates more efficient pressure transfer [56].

These results demonstrate that the fabricated PVDF sponges effectively function as piezoelectric structures capable of generating electrical signals in response to external stimuli. Moreover, the ability to control responsiveness and electrical output through pore structure tuning suggests that this approach can serve as a key strategic element in the design of biomaterials requiring electrophysiological stimulation.

5. CONCLUSION

In this study, we propose a simple yet highly reproducible fabrication process for porous PVDF piezoelectric sponges using compressed sugar cubes as pore-forming templates. Sugar serves as an effective template due to its tunable particle size and complete solubility during processing, enabling the formation of a continuous and uniform open-pore network within the structure. The use of molded sugar cubes as templates allowed for controlled pore size, ensured interconnectivity, and maintained structural uniformity, thereby addressing the issues of structural irregularity and low reproducibility commonly encountered in conventional porous fabrication techniques. The fabricated porous PVDF sponges exhibited distinct pore structures depending on the size of the sugar particles, which in turn led to differentiated performance in both mechanical properties and piezoelectric response. The continuity and openness of the internal pore architecture were visually confirmed through SEM and Micro-CT analyses, while tensile and compression tests validated the mechanical stability and strength of the structure. Furthermore, the PVDF sponge devices with integrated electrodes demonstrated stable electrical output under mechanical stimulation, confirming their functional effectiveness as piezoelectric materials.

This process can be implemented without the need for expensive equipment and enables precise control over pore structures using only common materials and a simple solution-based method, offering a practical strategy for improving process accessibility in the development of piezoelectric polymer-based porous architecture. It also fulfills key structural requirements for biomedical applications including controllable pore size, interconnectivity, mechanical robustness, and process reproducibility. Therefore, the sugar-cube templating approach and the resulting PVDF piezoelectric sponge developed in this study show strong potential as a platform technology for future high-performance piezoelectric

biomaterials, including implantable devices and tissue regeneration scaffolds.

ORCID

Chang Kyu Jeong https://orcid.org/0000-0001-5843-7609

ACKNOWLEDGEMENTS

This work was supported by the National Research Foundation of Korea (NRF) grants funded by the Ministry of Science, ICT and Future Planning (MSIT) (2022R1A2C4002037). This work was also supported by the Commercialization Promotion Agency for R&D Outcomes (COMPA) grant funded by the MSIT (RS-2023-00304743).

This research was supported by the Regional Innovation System & Education (RISE) initiative, funded by the Ministry of Education and administered by the National Research Foundation of Korea (NRF).

REFERENCES

[1] J. Choi, H. Kim, S. I. Yoon, and C. K. Jeong, *J. Korean Inst. Electr. Electron. Mater. Eng.*, **37**, 563 (2024).
doi: https://doi.org/10.4313/JKEM.2024.37.6.1

[2] Y. Song, T. Wu, J. Bao, M. Xu, Q. Yang, L. Zhu, Z. Shi, G. H. Hu, and C. Xiong, *Carbohydr. Polym.*, **288**, 119407 (2022).
doi: https://doi.org/10.1016/j.carbpol.2022.119407

[3] C. Nam, Y. Na, S. C. Park, H. Kim, C. K. Jeong, G. T. Hwang, and K. I. Park, *J. Mater. Chem. A*, **11**, 559 (2023).
doi: https://doi.org/10.1039/D2TA06171F

[4] Y. H. Jung, J. An, D. Y. Hyeon, H. S. Wang, I. Kim, C. K. Jeong, K. I. Park, P. S. Lee, and K. J. Lee, *Adv. Funct. Mater.*, **34**, 2309316 (2024).
doi: https://doi.org/10.1002/adfm.202309316

[5] Q. Xu, X. Gao, S. Zhao, Y. N. Liu, D. Zhang, K. Zhou, H. Khanbareh, W. Chen, Y. Zhang, and C. Bowen, *Adv. Mater.*, **33**, 2008452 (2021).
doi: https://doi.org/10.1002/adma.202008452

[6] J. Lee, S. Yoon, H. Kim, and C. K. Jeong, *J. Powder Mater.*, **32**, 16 (2025).
doi: https://doi.org/10.4150/jpm.2024.00444

[7] M. Ali, M. J. Bathaei, E. Istif, S. N. H. Karimi, and L. Beker, *Adv. Healthc. Mater.*, **12**, 2300318 (2023).
doi: https://doi.org/10.1002/adhm.202300318

[8] J. Park, Y. W. Lim, S. Y. Cho, M. Byun, K. I. Park, H. E. Lee, S. D. Bu, K. T. Lee, Q. Wang, and C. K. Jeong, *Small*, **18**, 2104472 (2022).
doi: https://doi.org/10.1002/smll.202104472

[9] S. Im, S. Y. Cho, J. H. Cho, G. T. Hwang, A. I. Kingon, S. D. Bu, W. Jo, S. H. Kim, and C. K. Jeong, *Appl. Surf. Sci.*, **613**, 156031 (2023).
doi: https://doi.org/10.1016/j.apsusc.2022.156031

[10] M. M. Abolhasani, M. Naebe, M. H. Amiri, K. Shirvanimoghaddam, S. Anwar, J. J. Michels, and K. Asadi, *Adv. Sci.*, **7**, 2000517 (2020).
doi: https://doi.org/10.1002/advs.202000517

[11] H. Kim, G. J. Lee, Y. Ogawa, Y. Lee, M. K. Lee, C. Baek, and C. K. Jeong, *Trans. Electr. Electron. Mater.*, **25**, 15 (2024).
doi: https://doi.org/10.1007/s42341-023-00500-5

[12] S. C. Park, C. Nam, C. Baek, M. K. Lee, G. J. Lee, and K. I. Park, *ACS Sustain. Chem. Eng.*, **10**, 14370 (2022).
doi: https://doi.org/10.1021/acssuschemeng.2c05026

[13] Y. Ma, H. Wang, Q. Wang, X. Cao, and H. Gao, *Chem. Eng. J.*, **452**, 139424 (2023).
doi: https://doi.org/10.1016/j.cej.2022.139424

[14] X. Cui, Y. Shan, J. Li, M. Xiao, Y. Xi, J. Ji, E. Wang, B. Zhang, L. Xu, M. Zhang, Z. Li, and Y. Zhang, *Adv. Funct. Mater.*, **34**, 2403759 (2024).
doi: https://doi.org/10.1002/adfm.202403759

[15] M. S. Park, M. J. Kim, J. Y. Jeong, D. Y. Han, S. Kim, G. T. Hwang, H. Yoo, and E. K. Lee, *Macromol. Res.*, **33**, 451 (2025).
doi: https://doi.org/10.1007/s13233-024-00341-y

[16] S. J. Yoon, H. Kim, C. K. Jeong, and Y. K. Lee, *J. Korean Ceram. Soc.*, **61**, 429 (2024).
doi: https://doi.org/10.1007/s43207-024-00369-x

[17] D. Xu, S. Fu, H. Zhang, W. Lu, J. Xie, J. Li, H. Wang, Y. Zhao, and R. Chai, *Adv. Mater.*, **36**, 2307896 (2024).
doi: https://doi.org/10.1002/adma.202307896

[18] Y. Chen, W. Xu, X. Zheng, X. Huang, N. Dan, M. Wang, Y. Li, Z. Li, W. Dan, and Y. Wang, *Biomacromolecules*, **24**, 1483 (2023).
doi: https://doi.org/10.1021/acs.biomac.2c01520

[19] O. Y. Dudaryeva, L. Cousin, L. Krajnovic, G. Gröbli, V. Sapkota, L. Ritter, D. Deshmukh, Y. Cui, R. W. Style, R. Levato, C. Labouesse, and M. W. Tibbitt, *Adv. Mater.*, **37**, 2410452 (2025).
doi: https://doi.org/10.1002/adma.202410452

[20] Y. Jin, J. Li, H. Fan, J. Du, and Y. He, *Small*, **21**, 2409955 (2025).
doi: https://doi.org/10.1002/smll.202409955

[21] L. Luo, W. Zheng, J. Li, T. Chen, W. Xue, T. Lin, M. Liu, Z. Yan, J. Yang, J. Li, J. Pu, Y. Wu, K. Hu, S. Li, and W. Huang, *Adv. Sci.*, **12**, 2500599 (2025).
doi: https://doi.org/10.1002/advs.202500599

[22] Q. Hou, D. W. Grijpma, and J. Feijen, *Biomaterials*, **24**, 1937 (2003).
doi: https://doi.org/10.1016/S0142-9612(02)00562-8

[23] P. Wang, H. Lv, X. Cao, Y. Liu, and D. G. Yu, *Polymers*, **15**, 921 (2023).
doi: https://doi.org/10.3390/polym15040921
[24] U.G.T.M. Sampath, Y. C. Ching, C. H. Chuah, J. N. Sabariah, and P. C. Lin, *Materials*, **9**, 991 (2016).
doi: https://doi.org/10.3390/ma9120991
[25] N. Thadavirul, P. Pavasant, and P. Supaphol, *J. Biomed. Mater. Res. A*, **102**, 3379 (2014).
doi: https://doi.org/10.1002/jbm.a.35010
[26] Q. Xing, X. Dong, R. Li, H. Yang, C. C. Han, and D. Wang, *Polymer*, **54**, 5965 (2013).
doi: https://doi.org/10.1016/j.polymer.2013.08.007
[27] C. J. Liao, C. F. Chen, J. H. Chen, S. F. Chiang, Y. J. Lin, and K. Y. Chang, *J. Biomed. Mater. Res.*, **59**, 676 (2002).
doi: https://doi.org/10.1002/jbm.10030
[28] Q. Cai, J. Yang, J. Bei, and S. Wang, *Biomaterials*, **23**, 4483 (2002).
doi: https://doi.org/10.1016/S0142-9612(02)00168-0
[29] M. H. Ho, P. Y. Kuo, H. J. Hsieh, T. Y. Hsien, L. T. Hou, J. Y. Lai, and D. M. Wang, *Biomaterials*, **25**, 129 (2004).
doi: https://doi.org/10.1016/S0142-9612(03)00483-6
[30] H. Matsuyama, Y. Takida, T. Maki, and M. Teramoto, *Polymer*, **43**, 5243 (2002).
doi: https://doi.org/10.1016/S0032-3861(02)00409-3
[31] Y. Yang, J. Zhao, Y. Zhao, L. Wen, X. Yuan, and Y. Fan, *J. Appl. Polym. Sci.*, **109**, 1232 (2008).
doi: https://doi.org/10.1002/app.28147
[32] H. Zhang and A. I. Cooper, *Adv. Mater.*, **19**, 1529 (2007).
doi: https://doi.org/10.1002/adma.200700154
[33] J. Grenier, H. Duval, P. Lv, F. Barou, C. Le Guilcher, R. Aid, B. David, and D. Letourneur, *Biomater. Adv.*, **139**, 212973 (2022).
doi: https://doi.org/10.1016/j.bioadv.2022.212973
[34] S. Mohanty, K. Sanger, A. Heiskanen, J. Trifol, P. Szabo, M. Dufva, J. Emnéus, and A. Wolff, *Mater. Sci. Eng. C*, **61**, 180 (2016).
doi: https://doi.org/10.1016/j.msec.2015.12.032
[35] T. K. Kim, J. J. Yoon, D. S. Lee, and T. G. Park, *Biomaterials*, **27**, 152 (2006).
doi: https://doi.org/10.1016/j.biomaterials.2005.05.081
[36] C. Zhou, K. Yang, K. Wang, X. Pei, Z. Dong, Y. Hong, and X. Zhang, *Mater. Des.*, **109**, 415 (2016).
doi: https://doi.org/10.1016/j.matdes.2016.07.094
[37] S. H. Oh, S. G. Kang, E. S. Kim, S. H. Cho, and J. H. Lee, *Biomaterials*, **24**, 4011 (2003).
doi: https://doi.org/10.1016/S0142-9612(03)00284-9
[38] D. Mao, Q. Li, D. Li, Y. Tan, and Q. Che, *Mater. Des.*, **160**, 1 (2018).
doi: https://doi.org/10.1016/j.matdes.2018.08.062
[39] M. Kim, S. Lee, and Y. Kim, *APL Mater.*, **8**, 071109 (2020).
doi: https://doi.org/10.1063/5.0011686
[40] O. B. Hassana, S. Guessasma, S. Belhabib, and H. Nouri, *Macromol. Mater. Eng.*, **301**, 566 (2016).
doi: https://doi.org/10.1002/mame.201500360
[41] S. Zhang, W. Feng, Y. Jiang, Y. Li, Y. Liu, D. Yu, and W. Wang, *Chem. Eng. J.*, **498**, 155356 (2024).
doi: https://doi.org/10.1016/j.cej.2024.155356
[42] H. Janik and M. Marzec, *Mater. Sci. Eng. C*, **48**, 586 (2015).
doi: https://doi.org/10.1016/j.msec.2014.12.037
[43] Y. Wan, N. Qin, Y. Wang, Q. Zhao, Q. Wang, P. Yuan, Q. Wen, H. Wei, X. Zhang, and N. Ma, *Chem. Eng. J.*, **383**, 123103 (2020).
doi: https://doi.org/10.1016/j.cej.2019.123103
[44] K. Lau, Y. Liu, H. Chen, and R. L. Withers, *Adv. Condens. Matter Phys.*, **2013**, 435938 (2013).
doi: https://doi.org/10.1155/2013/435938
[45] C. Thevenot, D. Rouxel, S. Sukumaran, S. Rouabah, B. Vincent, S. Chatbouri, and T. B. Zineb, *J. Appl. Polym. Sci.*, **138**, 50420 (2021).
doi: https://doi.org/10.1002/app.50420
[46] Y. Zhou, W. Liu, B. Tan, C. Zhu, Y. Ni, L. Fang, C. Lu, and Z. Xu, *Polymers*, **13**, 998 (2021).
doi: https://doi.org/10.3390/polym13070998
[47] Y. Jiang, L. Gong, X. Hu, Y. Zhao, H. Chen, L. Feng, and D. Zhang, *Polymers*, **10**, 364 (2018).
doi: https://doi.org/10.3390/polym10040364
[48] A. Arrigoni, L. Brambilla, C. Bertarelli, G. Serra, M. Tommasini, and C. Castiglioni, *RSC Adv.*, **10**, 37779 (2020).
doi: https://doi.org/10.1039/D0RA05478J
[49] J. Hou, J. Jiang, H. Guo, X. Guo, X. Wang, Y. Shen, and Q. Li, *RSC Adv.*, **10**, 10055 (2020).
doi: https://doi.org/10.1039/D0RA00956C
[50] H. Kashani, Y. Ito, J. Han, P. Liu, and M. Chen, *Sci. Adv.*, **5**, eaat6951 (2019).
doi: https://doi.org/10.1126/sciadv.aat6951
[51] S. K. Reddy, D. B. Ferry, and A. Misra, *RSC Adv.*, **4**, 50074 (2014).
doi: https://doi.org/10.1039/C4RA08321K
[52] Y. Chen, R. S. Carmichael, and T. B. Carmichael, *ACS Appl. Mater. Interfaces*, **11**, 31210 (2019).
doi: https://doi.org/10.1021/acsami.9b11149
[53] X. Zhang, J. Zhang, H. Sun, and Z. Wang, *J. Mater. Sci. Mater. Electron.*, **35**, 2210 (2024).
doi: https://doi.org/10.1007/s10854-024-13951-0
[54] Y. Chun and Y. G. Ko, *Compos. Commun.*, **53**, 102194 (2025).
doi: https://doi.org/10.1016/j.coco.2024.102194
[55] Z. Li, K. Hu, M. Yang, Y. Zou, J. Yang, M. Yu, H. Wang, X. Qu, P. Tan, C. Wang, X. Zhou, and Z. Li, *Nano Energy*, **58**, 852 (2019).
doi: https://doi.org/10.1016/j.nanoen.2018.11.093
[56] Y. S. Kim, Y. Xie, X. Wen, S. Wang, S. J. Kim, H. K. Song, and Z. L. Wang, *Nano Energy*, **14**, 77 (2015).
doi: https://doi.org/10.1016/j.nanoen.2015.01.006